

## X-Ray Imaging of Poly(Ethylene Glycol) Hydrogels Without Contrast Agents

Eric M. Brey, Ph.D.,<sup>1,2</sup> Alyssa Appel, M.S.,<sup>1,2</sup> Yu-Chieh Chiu, M.S.,<sup>1</sup> Zhong Zhong, Ph.D.,<sup>3</sup> Ming-Huei Cheng, M.D.,<sup>4</sup> Holger Engel, M.D.,<sup>4</sup> and Mark A. Anastasio, Ph.D.<sup>1</sup>

Hydrogels have shown promise for a number of tissue engineering applications. However, their high water content results in little or no image contrast when using conventional X-ray imaging techniques. X-ray imaging techniques based on phase-contrast have shown promise for biomedical application due to their ability to provide information about the X-ray refraction properties of samples. Nonporous and porous poly(ethylene glycol) hydrogels were synthesized and imaged using a synchrotron light source employing a silicon analyzer crystal and an X-ray energy of 40-keV. Data were acquired at 21 angular analyzer positions spanning the range of  $-5$  to  $5 \mu\text{rad}$ . Images that depict the projected X-ray absorption, refraction, and ultra-small-angle scatter (USAXS) properties of the hydrogels were reconstructed from the measurement data. The poly(ethylene glycol) hydrogels could be discerned from surrounding water and soft tissue in the refraction image but not the absorption or USAXS images. In addition, the refraction images of the porous hydrogels have a speckle pattern resulting in increased image texture in comparison to nonporous hydrogels. To our knowledge, this is the first study to show that X-ray phase-contrast imaging techniques can identify and provide detail on hydrogel structure without the addition of contrast agents.

### Brief Correspondence

**P**OLYMER HYDROGELS HAVE RECEIVED significant attention for applications in tissue engineering.<sup>1-3</sup> While these materials are being investigated in clinical and preclinical studies, it remains difficult to monitor their performance *in vivo*. An imaging technique that could identify hydrogels and provide structural information about the materials would be a significant advance in tissue engineering.

Hydrogels produce little or no image contrast when using conventional X-ray imaging techniques. Attempts to image hydrogels often rely on the introduction of contrast agents into the material.<sup>4</sup> These agents can influence cell behavior and material properties. The ideal system would allow material imaging without the addition of exogenous contrast agents. X-ray imaging techniques based on phase contrast<sup>5</sup> have shown promise for biomedical application due to their ability to provide information about soft tissue structure. In this communication, we examine an analyzer-based X-ray phase-contrast imaging method<sup>6-8</sup> for identifying hydrogels without the use of contrast agents.

Nonporous and porous (mean pore size =  $50 \pm 1$  and  $74 \pm 3 \mu\text{m}$ ) 25% (w/v) poly(ethylene glycol) (PEG) hydrogels were synthesized.<sup>9</sup> The samples were imaged without exogenous contrast agents at the X-15A beamline at the National Synchrotron Light Source at Brookhaven National Laboratories.<sup>10</sup> Hydrogels were imaged before implantation and after 1 week of subcutaneous implantation in a rat.<sup>11</sup> A silicon analyzer crystal employing a (3,3,3) reflection and an X-ray energy of 40 keV was employed. Data were acquired at 21 angular analyzer positions from  $-5$  to  $5 \mu\text{rad}$ . Images that depict the projected X-ray absorption, refraction, and ultra-small-angle scatter (USAXS) properties of the hydrogels were reconstructed from the measurement data.<sup>7</sup>

The hydrogels can be discerned from the surrounding water in the X-ray refraction images but not the absorption (Fig. 1) or USAXS (not shown) images. The refraction images of the porous hydrogels have a speckle pattern possibly resulting from multiple refractions of the beam as it passes through the pores. Measures of image texture<sup>12</sup> indicate that there is increased texture in the porous gels in comparison to

<sup>1</sup>Department of Biomedical Engineering, Illinois Institute of Technology, Chicago, Illinois.

<sup>2</sup>Hines Veterans Administration Hospital, Hines, Illinois.

<sup>3</sup>National Synchrotron Light Source, Brookhaven National Laboratory, Upton, New York.

<sup>4</sup>Department of Plastic and Reconstructive Surgery, College of Medicine, Chang Gung University, Chang Gung Memorial Hospital, Taoyuan, Taiwan.

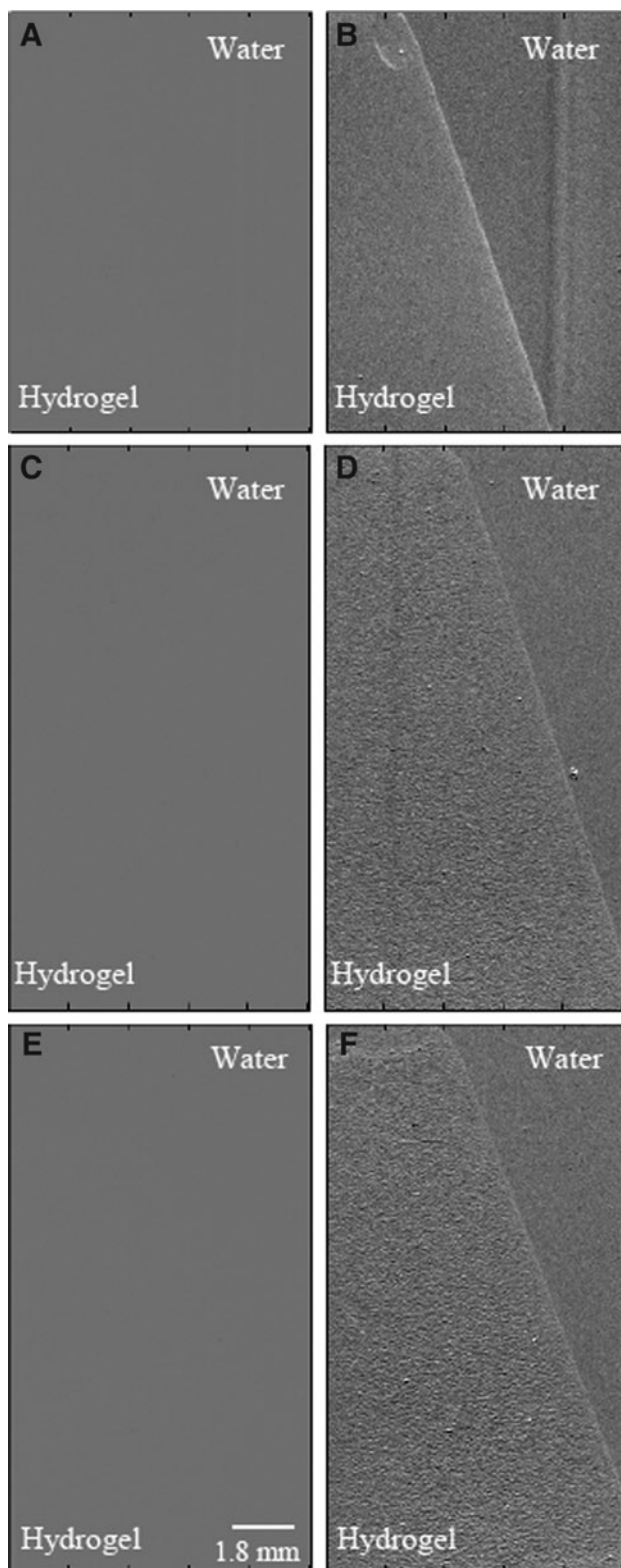


**FIG. 1.** X-ray refraction but not absorption allows identification of PEG hydrogels in water. (A), (C), and (E) are the absorption images of nonporous, porous (50  $\mu\text{m}$ ), and porous (74  $\mu\text{m}$ ) hydrogels, respectively. (B), (D), and (F) are the corresponding refraction images at the same location. PEG, poly(ethylene glycol).

**TABLE 1.** MEASURES OF TEXTURE IN X-RAY REFRACTION IMAGES OF HYDROGELS *IN VITRO*

	Mean intensity, $\mu = \sum_{i=0}^{L-1} z_i p(z_i)$	Standard deviation, $\sigma = \sqrt{\sum_{i=0}^{L-1} (z_i - \mu)^2 p(z_i)}$	Relative smoothness, $R = 1 - \frac{1}{1 + \sigma^2}$	Uniformity, $U = \sum_{i=0}^{L-1} p^2(z_i)$	Entropy, $E = - \sum_{i=0}^{L-1} p(z_i) \log_2 p(z_i)$
Nonporous	0.521	0.0309	0.0001	0.0358	5.02
Porous (50 $\mu\text{m}$ )	0.516	0.0725 <sup>a</sup>	0.0054	0.0161 <sup>a</sup>	6.22 <sup>a</sup>
Porous (74 $\mu\text{m}$ )	0.515	0.0667 <sup>a</sup>	0.0045 <sup>a</sup>	0.0167 <sup>a</sup>	6.13 <sup>a</sup>

<sup>a</sup>Indicates statistically significant differences ( $p < 0.05$  analysis of variance with Tukey post test) from nonporous  $z$ ,  $p(z)$ , and  $L$  denote intensity level, probability of intensity level, and number of intensity levels, respectively.

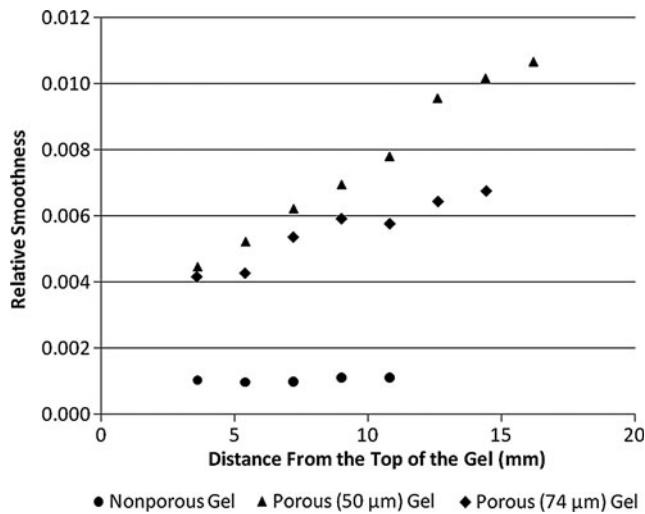


FIG. 2. Image texture (relative smoothness) increases with sample thickness for porous gels. Plot of relative smoothness versus distance from the top of the gel. The diameter of the gels increases as you move from the top to the bottom of the gel. The texture of the nonporous gel remains constant, whereas the texture of porous gels increases.

nonporous (Table 1). Interestingly, the texture measures increase with thickness of the porous hydrogels (Fig. 2) possibly due to increased extent of refractions as an increasing number of pores are encountered.

X-ray refraction images also allowed identification of the interface between hydrogels and fibrovascular tissue in explanted samples (Fig. 3). PEG and surrounding tissue are not visible in absorption nor USAXS images. Texture measurements were constant for all implanted hydrogels (Table 2). This may be due to soft tissue within the pores or imaging thinner ( $\sim 1$  mm) hydrogels resulting in an insufficient number of pores to generate the speckle pattern.

### Conclusions

These results establish that X-ray phase-contrast imaging techniques can reveal features of PEG hydrogels. To our knowledge, this is the first study to show that synthetic hydrogels can be imaged using an X-ray-based technique. X-ray imaging techniques have enjoyed significant interest in tissue engineering due to the high absorption contrast of hard tissues and injected agents.<sup>13</sup> These results suggests that X-ray phase contrast could further benefit tissue engineering by allowing imaging of hydrogels in engineered tissues.

### Acknowledgments

The research has been supported by the Veterans Administration, the National Science Foundation (0854430, 0731201, 0546113), the National Institute of Health (R01E B009715), and Chang Gung Memorial Hospital (CMRPG 390101).

### Disclosure Statement

No competing financial interests exist.

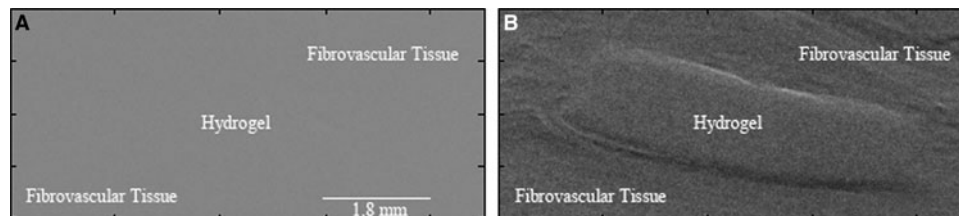


FIG. 3. X-ray refraction but not absorption allows identification of the interface between PEG hydrogels and surrounding fibrovascular tissue. (A) Absorption and (B) refraction images of porous ( $74 \mu\text{m}$ ) PEG hydrogels after 1 week of implantation. The images are from the same tissue location.

TABLE 2. MEASURES OF TEXTURE IN X-RAY REFRACTION IMAGES OF HYDROGELS AFTER 1 WEEK OF IMPLANTATION

	Mean intensity, $\mu = \sum_{i=0}^{L-1} z_i p(z_i)$	Standard deviation, $\sigma = \sqrt{\sum_{i=0}^{L-1} (z_i - \mu)^2 p(z_i)}$	Relative smoothness, $R = 1 - \frac{1}{1 + \sigma^2}$	Uniformity, $U = \sum_{i=0}^{L-1} p^2(z_i)$	Entropy, $E = - \sum_{i=0}^{L-1} p(z_i) \log_2 p(z_i)$
Nonporous	0.597	0.0370	0.0014	0.0302	5.28
Porous ( $50 \mu\text{m}$ )	0.457	0.0391	0.0015	0.0285	5.36
Porous ( $74 \mu\text{m}$ )	0.459	0.0344	0.0012	0.0327	5.17

$z$  denotes intensity level,  $p(z)$  denotes probability of intensity level, and  $L$  denotes number of intensity levels.

## References

1. Hoffman, A.S. Hydrogels for biomedical applications. *Adv Drug Deliv Rev* **54**, 3, 2002.
2. Lutolf, M.P., and Hubbell, J.A. Synthetic biomaterials as instructive extracellular microenvironments for morphogenesis in tissue engineering. *Nat Biotechnol* **23**, 47, 2005.
3. Chiu, Y.C., Cheng, M.H., Uriel, S., and Brey, E.M. Materials for engineering vascularized adipose tissue. *J Tissue Viability* 2010 [Epub ahead of print].
4. Faraj, K.A., Cuijpers, V.M., Wismans, R.G., Walboomers, X.F., Jansen, J.A., van Kuppevelt, T.H., and Daamen, W.F. Micro-computed tomographical imaging of soft biological materials using contrast techniques. *Tissue Eng Part C Methods* **15**, 493, 2009.
5. Lewis, R. Medical phase contrast X-ray imaging: current status and future prospects. *Phys Med Biol* **49**, 3573, 2004.
6. Wernick, M.N., Wirjadi, O., Chapman, D., Zhong, Z., Galatsanos, N.P., Yang, Y., Brankov, J.G., Oltulu, O., Anastasio, M.A., and Muehleman, C. Multiple-image radiography. *Phys Med Biol* **48**, 3875, 2003.
7. Chou, C.Y., Anastasio, M.A., Brankov, J.G., Wernick, M.N., Brey, E.M., Connor, D.M., and Zhong, Z. An extended DEI method for implementing multiple-image radiography. *Phys Med Biol* **52**, 1923, 2007.
8. Brankov, J.G., Wernick, M.N., Yang, Y., Li, J., Muehleman, C., Zhong, Z., and Anastasio, M.A. A computed tomography implementation of multiple-image radiography. *Med Phys* **33**, 278, 2006.
9. Chiu, Y.C., Larson, J.C., Isom, A., and Brey, E.M. Generation of porous poly(ethylene glycol) hydrogels by salt leaching. *Tissue Eng Part C Methods* 2010 (In press).
10. Zhong, Z., Thomlinson, W., Chapman, D., and Sayers, D.E. Implementation of diffraction enhanced imaging experiments: at the NSLS and APS. *Nucl Instrum Methods Phys Res A* **450**, 556, 2000.
11. Brey, E.M., King, T.W., Johnston, C., McIntire, L.V., Reece, G.P., and Patrick, C.W., Jr. A technique for quantitative three-dimensional analysis of microvascular structure. *Microvasc Res* **63**, 279, 2002.
12. Haralick, R.M., Dinstein, I., and Shanmuga, K. Textural features for image classification. *IEEE Trans Syst Man Cybern* **3**, 610, 1973.
13. Young, S., Kretlow, J.D., Nguyen, C., Bashoura, A.G., Baggett, L.S., Jansen, J.A., Wong, M., and Mikos, A.G. Microcomputed tomography characterization of neovascularization in bone tissue engineering applications. *Tissue Eng Part B Rev* **14**, 295, 2008.

Address correspondence to:

*Eric M. Brey, Ph.D.*

*Department of Biomedical Engineering*

*Illinois Institute of Technology*

*3255 South Dearborn St.*

*Chicago, IL 60616*

*E-mail: brey@iit.edu*

*Received: March 22, 2010*

*Accepted: June 15, 2010*

*Online Publication Date: July 21, 2010*